



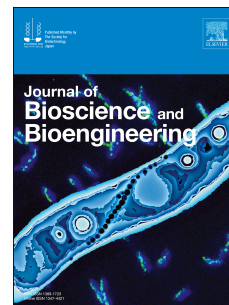
Since January 2020 Elsevier has created a COVID-19 resource centre with free information in English and Mandarin on the novel coronavirus COVID-19. The COVID-19 resource centre is hosted on Elsevier Connect, the company's public news and information website.

Elsevier hereby grants permission to make all its COVID-19-related research that is available on the COVID-19 resource centre - including this research content - immediately available in PubMed Central and other publicly funded repositories, such as the WHO COVID database with rights for unrestricted research re-use and analyses in any form or by any means with acknowledgement of the original source. These permissions are granted for free by Elsevier for as long as the COVID-19 resource centre remains active.

Journal Pre-proof

Development of Nucleic Acid Based Lateral Flow Assays for SARS-CoV-2 Detection

Dilek Çam Derin, Enes Gültekin, Irmak İçen Taşkın, Yusuf Yakupoğulları



PII: S1389-1723(22)00340-1

DOI: <https://doi.org/10.1016/j.jbiosc.2022.11.001>

Reference: JBIOSC 3150

To appear in: *Journal of Bioscience and Bioengineering*

Received Date: 30 August 2022

Revised Date: 24 October 2022

Accepted Date: 1 November 2022

Please cite this article as: Çam Derin D, Gültekin E, İçen Taşkın I, Yakupoğulları Y, Development of Nucleic Acid Based Lateral Flow Assays for SARS-CoV-2 Detection, *Journal of Bioscience and Bioengineering*, <https://doi.org/10.1016/j.jbiosc.2022.11.001>.

This is a PDF file of an article that has undergone enhancements after acceptance, such as the addition of a cover page and metadata, and formatting for readability, but it is not yet the definitive version of record. This version will undergo additional copyediting, typesetting and review before it is published in its final form, but we are providing this version to give early visibility of the article. Please note that, during the production process, errors may be discovered which could affect the content, and all legal disclaimers that apply to the journal pertain.

© 2022, The Society for Biotechnology, Japan. All rights reserved.

Development of Nucleic Acid Based Lateral Flow Assays for SARS-CoV-2 Detection

Dilek Çam Derin^{a*}, Enes Gültekin^b, Irmak İçen Taşkın^c, Yusuf Yakupoğulları^d

^{a,b,c} Inonu University, Department of Molecular Biology and Genetics, 44280, Malatya, Turkey

^d Inonu University, Department of Medical Microbiology, 44280, Malatya, Turkey

*Corresponding author: cam.dilek@gmail.com, Phone number: +90 422 377 30 00

Short title: Molecular detection of 2019-nCoV_N3

ABSTRACT

SARS-CoV-2 is still threat for humanity and its detection is crucial. Although real time reverse transcriptase polymerase chain reaction is the most reliable method for detection of N protein genes, alternative methods for molecular detection is still needed. Thus, lateral flow assay models for 2019-nCoV_N3 were developed for molecular detection. Briefly, gold nanoparticles were used as label and three sandwich models (1A, 1B, 1.2) were designed. Prob concentrations on gold nanoparticles, types of sandwich model and membrane, limit of detection of target gene and buffer efficiency were studied. Model 1B has shown the best results with M170 membrane. Lower limit of detection was achieved by model 1.2 as 5pM. All parameters have significant role for molecular detection of SARS-CoV-2 by lateral flow assays, and these results will be useful for nucleic acid based lateral flow assays for viral detection or multiple detection of mutated forms in various detection systems.

Keywords

rapid test, SARS-CoV-2, sandwich assay, 2019-nCoV_N, detection

INTRODUCTION

27 Wuhan Viral Pneumonia seen in the late 2019 was called as SARS-CoV-2 and COVID-19
28 caused by SARS-CoV-2 was named as disease by World Health Organization (WHO). SARS-
29 CoV-2 is an RNA virus belonging to the β and it has at least four structural proteins including
30 Spike (S) protein, envelope (E) protein, membrane (M) protein and nucleocapsid (N) protein.
31 S protein is widely used for diagnosis because of antigenicity and commonly chosen as target
32 for neutralizing antibodies. However, N protein become attractive for molecular diagnosis of
33 COVID-19 as highly protected protein sequences and high immunogenicity (1). Additionally,
34 N protein is abundantly expressed protein during the infection and causes to protective immune
35 response for SARS CoV and COVID-19 (2). The sequence similarity of protein coding region
36 of COVID-19 was found as 89.74%, 48.59% and 35.62% with SARS CoV, MERS-CoV and
37 HCoV-OC43, respectively (3) and 96% with bat coronavirus in the whole genom level (1).
38 Comprehensive domain structure of N proteins among the four coronaviruses (SARS-CoV-2,
39 SARS-CoV, MERS-CoV, and HCoV-OC43) and complete genome of SARS-CoV-2 were
40 reported in the literature respectively (3). To say that the characteristics of the surface
41 electrostatic potential of N terminal domain of SARS-CoV-2 N protein is different even if it is
42 similar to the other coronaviruses.

43

44 N region of SARS-CoV-2 was determined as target sequence for SARS-CoV-2 specific gene.
45 WHO proposed a few primer sets for N gene and reported that 2019-nCoV_N3 (USA) and
46 NIID_2019-nCoV_N (Japan) primers are the most sensitive for real time reverse transcription
47 polymerase chain reaction (rRT-PCR) respectively (4). Therefore, among the specific regions
48 N gene regions are widely accepted for diagnosis as the high similarity between SARS-CoV-2
49 and SARS-CoV causes to mistake in molecular diagnosis. SARS-CoV-2 RNA may be obtained
50 from bronchoalveolar lavage, nasal/pharyngeal swab (53.6% - 73.3%) (5), salivary/sputum
51 (74.4%-88.9%) (6), feces/urine, blood samples and anal/oral swabs (7-9). Additionally, it is

52 known that virus may be alive at suitable environmental conditions after leaving from human
53 body and join to waste water. Thus, SARS-CoV-2 and newly developed coronaviruses will
54 always threaten the public health since the development of antiviral drugs or therapeutics takes
55 long time. In this reason, early molecular viral detection is crucial to get under control the
56 epidemy/pandemia.

57

58 Serology is a standart method for viral detection and based on the testing of antibody response
59 coming from the immune system and antigen presence. However, it cannot be used for early
60 detection since it is based on the measurement of antibody after infection, and could not be
61 efficient for patients who are in risk groups. For instance, antibodies against to COVID-19 are
62 developed in early stage (4-10 days for IgM) and late stage (11-24 days for IgM-IgG). Besides,
63 cross antibody reactions may give a false positive result and producing of polyclonal antibodies
64 may change from batch to batch. Nanoparticle based viral diagnosis (10) is another way and it
65 was used for the detection of SARS specific sequence (11). However, there is lack of nano-
66 based diagnosis systems for SARS-CoV-2 sequences even if antigen based detections are
67 reported (12-17). rRT-PCR is the most reliable method for molecular detection of SARS-CoV-
68 2 in the world and the first quantitative rRT-PCR was designed after the definition of virus by
69 WHO in January 2020 (<https://www.who.int/emergencies/diseases/novel-coronavirus>).
70 Although these assays are reliable, complex and expensive test protocols, need of educated
71 personnel and diagnosis laboratories, taking time for sending the samples into reference labs
72 are disadvantages. Similarly, conventional PCR needs to agarose gel loading and high copy
73 number of target genes. For this reasons, rapid and naked eye molecular detection of SARS-
74 CoV-2 is always be needed. In this regard, lateral flow assays (LFAs) or point of care tests could
75 be an alternative to the molecular detection of SARS-CoV-2 as a rapid, cheap and simple way
76 without advanced devices in a short time.

77 LFAs are portable, ready to use immunochromatographic diagnostic assays developed by
78 antibodies, enzymes or nucleic acids (18) for various fields. They can also be helpful for
79 epidemy/pandemia by sensitive detection of nucleic acids (19) and could make 8 times sensitive
80 and rapid detection compared to the electrophoresis (20). While a number of LFAs were
81 developed for COVID-19 they are mostly based on the antibody (IgG/IgM) detection of patients
82 (21) and there is lack of nucleic acid detection of SARS-CoV-2 by LFAs. LFAs can be used
83 with amplification systems producing any RNA (22). Although LFA for molecular detection of
84 SARS-CoV-2 is reported in the literature it is based on CRISPR Cas12a dependent nucleic acid
85 detection (23) and needs the complex experimental steps. Similarly, Broughton et al., developed
86 the LFAs for SARS-CoV-2 using the RNA extracts related with respiratory swab. It is based on
87 the CRISPR–Cas12 for the detection of E and N gene (24). However, extra labelling with
88 Fluorescein amidites and sensitive steps including enzymatic restriction are needed, and assay
89 was only developed for one region of N gene announced by US Centers for Disease Control
90 and Prevention ([https://www.cdc.gov/coronavirus/2019-ncov/lab/rt-pcr-detection-](https://www.cdc.gov/coronavirus/2019-ncov/lab/rt-pcr-detection-instructions.html)
91 [instructions.html](https://www.cdc.gov/coronavirus/2019-ncov/lab/rt-pcr-detection-instructions.html)) which are accepted regions for rRT-PCR. LFAs are encouraged to be
92 developed for nucleic acid detection of SARS-CoV-2 based on PCR. Therefore, nucleic acid
93 based LFAs are always become crucial and they can be adopted the new sequences occurred by
94 mutations in the virus.

95

96 In this research, molecular detection of RNA region (2019-nCoV_N3) specific to SARS-CoV-
97 2 by gold nanoparticles (AuNPs) based LFAs in 5-7 minutes was aimed. Test principle is based
98 on the hybridization of oligonucleotides without complex enzymatic reactions and naked eye
99 analysis.

100

101 **MATERIALS AND METHODS**

102 The chemicals used were all analytical grades. HAuCl₄. 3H₂O, trisodium citrate dihydrate were
103 purchased from Alfa Aesar (Kandel, Germany). Ultra-low range DNA ladder were from
104 Thermo Scientific. Tris-HCl was purchased from Applichem, KCl and NaCl were purchased
105 from Merck, MgCl₂, CaCl₂, nuclease free water and SSC buffer were purchased from Multicell.
106 Tris(2-carboxyethyl)phosphine hydrochloride (TCEP) was purchased from Sigma Aldrich.
107 Synthetic oligonucleotides were purchased from Integrated DNA Technologies (Coralville,
108 USA). Ultrapure water was used for the preparation of all solutions during the study. The
109 nitrocellulose membrane cards were purchased from Whatman, Germany. Absorbent pad,
110 sample pad and conjugate pad were purchased from Millipore, USA. Scanning transmission
111 electron microscope (STEM-TESCAN), HORIBA Dynamic Laser Particle Size/Zeta Potential
112 Analyzer and EPOCH2 Plate Reader/Spectrophotometer were used for analysis of synthesized
113 AuNPs and AuNPs/prob concentration. As a probe 1A model: GNP probe 1A: 5' cca atg tga tct
114 ttt ggt gta aaa aaa aaa-3 -SH'; test line for 1A: 5'bio aaa aaa a gca ttg tta gca gga ttg c 3' and
115 control line for 1A: 5' tac acc aaa aga tca cat tgg ttt 3'bio were used. As a probe 1B model: GNP
116 probe 1B: 5' ttt ggt gta ttc aag gct ccc aaa aaa aaa-3 -SH'; test line for 1B: 5'bio aaa aaa tg cgg
117 gtg cca atg tga tct 3' and control line for 1B: 5' ggg agc ctt gaa tac acc aaa ttt 3'bio were used.
118 As a probe 1.2 model: GNP probe 1.2: 5' t gcc aat gtg atc ttt tgg tg aaa aaa aaa-3 -SH'; test line
119 for 1.2: 5'bio aaa aaa gc agc att gtt agc agg att 3' and control line for 1.2: 5' ca cca aaa gat cac
120 att ggc a ttt 3'bio were used. 72 base long target N gene region 1 (2019-nCoV_N3), 5'-ggg agc
121 ctt gaa tac acc aaa aga tca cat tgg cac ccg caa tcc tgc taa caa tgc tgc aat cgt gct aca-3', and 50
122 base long target N gene region 1.2 (2019-nCoV_N3), 5' aat aca cca aaa gat cac att ggc acc cgc
123 aat cct gct aac aat gct gc -3', were experienced. 5'ggg agc ctt gaa tac acc aaa a 3' and 5'tgt agc
124 acg att gca gca ttg 3' primers were used as forward and reverse, respectively for PCR reaction.

125

126 **Synthesis of Gold Nanoparticles and Conjugation with oligonucleotide probes**

127 AuNPs were synthesized by reducing the $\text{HAuCl}_4 \cdot 3\text{H}_2\text{O}$ with sodium citrate (25), in conical
128 flask. All the glass materials used were cleaned with acid solution and rinsed with distilled water.
129 Briefly, 100 mL of 1mM $\text{HAuCl}_4 \cdot 3\text{H}_2\text{O}$ solution was boiled by stirring continuously. Then 1%
130 sodium citrate was added and the color changed from black to red in 2-3 minutes. Boiling was
131 continued about 10 minutes and colloidal solution was allowed to cool. Synthesized AuNPs
132 were filtered by 0.45 μm cellulose acetate and concentrated by centrifugation at four times (4X
133 AuNPs) before the conjugation with oligonucleotides and stored at 4°C. To make a conjugate
134 with oligonucleotide probes, thiol modified probes were initially activated by TCEP for one
135 hour at room temperature. In this purpose, three probe concentrations (2 μM , 4 μM , 8 μM) were
136 used for conjugation in order to see the effect of probe concentration on assay efficiency. Then
137 solution was added into 1 ml of 4X AuNPs solution and incubated for overnight at room
138 temperature. After that 0.01M phosphate buffer saline (PBS) was added as final concentration
139 for salt aging and incubated for overnight. Then, the solution was centrifuged at 12000 rpm and
140 pellet was resuspended in resuspension buffer (20mM sodium phosphate buffer containing 5%
141 BSA, 0.25 % Tween 20 and sucrose). Conjugate was washed with the resuspension buffer as
142 twice and stored at 4°C after resuspending in the same buffer.

143

144 **Preparation of LFAs**

145 The components of the LFAs are sample pad, conjugate pad, nitrocellulose membrane and
146 absorbent pad. The design of strip assay was manually performed according to our previous
147 study (26). Two different cellulose membranes having different flow rates were used in this
148 study (M170-M120). In short, sample pads were treated with two different buffers called as
149 buffer 4 (0.05M Tris-HCl, 0.25% Triton X 100, 0.15M NaCl, pH 8.0) and buffer 5 (PBS,
150 0.1mM NaCl, 0.2 % Tween 20), separately and dried at 37°C or room temperature. Conjugate

151 pads were soaked with AuNPs/Probe conjugate and dried at 37°C for 1 hour. Buffer 14 (20mM
152 Tris, 50mM NaCl, 5mM KCl, 5mM MgCl₂, 2mM CaCl₂, 0.1mM BSA, 1.7% Triton X 100,
153 pH 8.0), PBS and saline-sodium citrate (SSC) was used as running buffer for optimizing the
154 assay. Test and control lines are prepared by the principle of streptavidin-biotin interaction.
155 Briefly, biotinylated oligonucleotides were conjugated to streptavidin and then immobilized on
156 the cellulose membrane using micropipette, manually. For the assay development three
157 sandwich models (1A, 1B, 1.2) were prepared for hybridization on LFA and experienced,
158 separately. Two of them (1A, 1B) were for 72 base long 2019-nCoV_N3 and the last one (1.2)
159 was for 50 base long which was obtained from shortening the 2019-nCoV_N3 region which is
160 still specific for SARS-CoV-2.

161

162 **Polimerase Chain Reaction for 2019-nCoV_N3**

163 In order to see the application potential of developed LFAs for real samples, PCR was
164 performed by plasmid DNA including N gene of SARS-CoV-2 and specific primers for 2019-
165 nCoV_N3. After the reaction was completed, PCR product was run on agarose gel
166 electrophoresis along with the Ultra-low DNA ladder at 90V for 1 hour to be sure that correct
167 gene region was obtained before applying to the LFA. The PCR reaction was performed as 34
168 cycle for each tube and finally extended as 72°C for 4 minute. PCR products were heated for
169 denaturation and then applied to the strip assays.

170

171 **RESULTS AND DISCUSSION**

172 **Synthesis of Gold Nanoparticles and Conjugation with oligonucleotide probes**

173 Synthesized AuNPs were analyzed by STEM, UV-Vis spectroscopy and Dynamic Laser Particle
174 Size Analyzer. According to the analysis, homogenously distributed spherical colloidal AuNPs
175 were measured as about 13 nm and λ_{\max} was 521 nm as expected (Fig. S1). Additionally, the

176 measurement of STEM analysis showed that Value: 1 [nm], Obj. count: 85, Summation: 1071.01,
177 Min. value: 9.44, Max. value: 20.26, Mean value: 12.60 and Std. dev. :2.21. The concentration
178 of synthesized AuNPs was also calculated as 0.4nM according to the extinction coefficient of
179 13 nm at 521 nm wavelength (27).

180

181 After the conjugation of AuNPs with thiol modified probes their max absorption peaks were
182 shifted from 521 nm to 526 nm as expected (Fig. S2). Because coating of AuNPs by probes
183 (4 μ M, 8 μ M) for three sandwich models caused the changing of surface charges of AuNPs and
184 resulted with max absorption peak shift. While the concentration of probes on AuNPs was
185 enough for 4 μ M and 8 μ M for three models, 2 μ M probe was not enough for sustaining the
186 stability of AuNPs since it caused the aggregation of AuNPs (data not shown). Therefore, 4 μ M
187 and 8 μ M coated AuNPs were used for further studies for three LFA models.

188

189 **Preparation of LFA models**

190 The components of LFAs were manually prepared and three sandwich models (1A, 1B, 1.2)
191 (Fig. S3) were applied to assay, separately. These models were designed to make comparison
192 between the models and find the best one for molecular recognition of SARS-CoV-2 by LFAs.

193

194 **Agarose Gel Electrophoresis of 2019-nCoV_N3 PCR**

195 PCR was performed by using plasmid DNA including N gene and primers specific for 2019-
196 nCoV_N3 were used for amplification of 72bp target. This was made for verification of
197 presenting the target gene in our sample and mimicking the real PCR samples coming from the
198 patients, which will be applied to the LFAs for further studies. PCR products for 2019-
199 nCoV_N3 (72 bp) was shown in Fig. S4.

200

201 **Application of targets to the LFAs models**

202 Here probe concentration on AuNPs, sandwich models, membrane types, limit of detection
203 (LOD) of target gene and buffer efficiency for molecular detection of 2019-nCoV_N3 on
204 designed LFAs were studied. LFAs were prepared by four membranes and target was used as
205 synthetic oligonucleotide sequence of 2019-nCoV_N3. Initially, buffer optimizations were
206 experienced. For this purpose, sample pads were soaked with two buffers, buffer 4 and buffer
207 5, and three different buffers, buffer 14, PBS and SSC were used as running buffer. In these
208 conditions the control lines of LFAs should always be seen as red and in order to say that test
209 is positive both the test and control line should be seen as red. Results verified that membrane
210 type and designed models have significant differences when they are used with different buffers
211 and temperatures (data not shown). For instance, model 1B has shown the best results with
212 M170 membrane compared to the M120 membrane for using 4 μ M and 8 μ M probe
213 concentrations at 37°C drying (Fig. 1, B1-B10; D1-D4), while the model 1A has weak test lines
214 with M170 and M120 membranes at the same temperature (Fig. 1, A1-A10; C1-C4). Although
215 there are no significant differences between buffer 4 and 5 for assay results, SSC buffer was
216 used for further studies as it has clear red color intensity on both the test and control lines and
217 showed no nonspecific bindings on LFAs for all models using 4 μ M and 8 μ M probe
218 concentrations. This finding is meaningful as SSC buffer has commonly positive effect on
219 oligonucleotide hybridizations. To highlight, all developed strips have selectively detected the
220 target and showed no nonspecific binding to the Mers CoV_N2, Mers CoV_N3 and RdRp/Orf1
221 sequences of SARS CoV_2, which are specific for Mers CoV and SARS-CoV-2, respectively.
222 This means that designed LFA strips are suitable and usable for the molecular detection of
223 SARS-CoV-2, reliably. Additionally, all strip assays worked truly since all the control lines are
224 visible even if two of them are weak in positive assay (Fig. 1, A1,C1). This is probably caused
225 by the weak interaction between the capture and detection reagent for prob 1A.

226 **Application of PCR products to LFAs designed by three models**

227 PCR products were applied to the developed LFAs using three models and two type of
228 membranes. To make sure that for selective detection of target, random oligonucleotide
229 sequences such as Se20_60 bio, Crn2SH and Mers CoV_N2, Mers CoV_N3 and RdRp/Orf1 of
230 SARS-CoV-2, SSC running buffer were used as negative controls. Findings showed that all
231 models recognized the target sequence, selectively without any nonspecific bindings of negative
232 controls (Fig. 2). Although there is no significant differences between the strip assays, model
233 1B on both membranes might be considered as the best for the detection of 2019-nCoV_N3 in
234 PCR sample by two probe concentrations (Fig. 2 strip 6, 8, 11, 16). Although the test line
235 intensity on model 1.2 (Fig. 2, A1) and model 1A (Fig. 2, B14-B15) is weak compared to model
236 1B they could make selective detection without any nonspecific binding to the negative controls
237 (Fig. 2, A2-A5, Fig. 1, A, C).

238
239 Briefly, all these results mean that designed assay models could be good candidate for naked
240 eye analysis of SARS-CoV-2 without needed advanced rRT-PCR devices and agarose gel
241 electrophoresis. Additionally, as very low amount of PCR product, 5 μ L, is loaded on developed
242 LFAs it seems advantageous and sensitive compared to the traditional agarose gel
243 electrophoresis. Because agarose gel electrophoresis needs to the high amount of PCR product
244 and long time for analysis. To highlight, there is no significant difference between two probe
245 concentrations (4 μ M-8 μ M) for detection of PCR products.

246

247 **Limit of Detection of LFAs designed by three models**

248 LOD experiments were performed by using synthetic target with developed LFAs by three
249 sandwich models and both membrane types. It is clearly seen that model 1A works efficiently
250 since the control lines of all strips are seen and results showed that 0.1 μ M target, 72 base long,

251 was sensitively recognized by model 1A using both membrane types (Fig. 3, B3 and D1, D3).
252 Interestingly, there is significant difference in terms of the detection of this amount by M120
253 membrane. The line intensities of 0.5 μ M target (Fig. 3, C) are weak compared to the 0.1 μ M
254 target (Fig. 3, D).

255
256 It might be said that the sensitivity of LFAs based on hybridization is significantly affected by
257 the amount of target and membrane type. It means that there is an optimum concentration
258 between the capture and detection oligonucleotides for effective hybridization and it is not
259 directly related with high amount of target for this model designed with this membrane.
260 However, the line intensities on M170 membrane were gradually become weak when the
261 concentration of target was decreased for two probe concentrations (Fig. 3, A-B). While the
262 LOD is 0.1 μ M target by using 8 μ M probe (Fig. 3, B3), it was 0.5 μ M using 4 μ M probe on this
263 membrane. These findings suggested that probe concentrations on AuNPs has significant role
264 for sensitive detection along with the membrane type. This can also be verified by comparing
265 the strips developed by 4 μ M probes with M170 (Fig. 3, B1) and M120 membrane (Fig. 3, D1)
266 for the same LOD.

267
268 LOD experiments were experienced by model 1B using both membranes and two probe
269 concentrations (Fig. 4). According to the results 0.1 μ M target, 72 base long, was detected by
270 M170 membrane using both probe concentrations (Fig. 4, B) while it was 0.005 μ M by M120
271 membrane using 8 μ M probe (Fig. 4, F). These results verified that membrane types and probe
272 concentrations used in LFAs have significant role for sensitive detection. Here, used sandwich
273 model, another important point for sensitive detection, seems better than model 1A since the all
274 strips have clear line intensities and lower detection limit.

275

276 LOD was also experienced by model 1.2 using both membranes and two probe concentrations
277 (Fig. 5). According to the results the minimum amount of target, 50 base long, was detected as
278 5pM by M170 membrane using 8 μ M probe (Fig. 5, C1) while it was 100pM by M120
279 membrane using 8 μ M probe concentration (Fig. 5, E3) without any nonspecific bindings. This
280 amount is either lower than the reported nucleic acid based LFAs (28,29) or similar with the
281 amount of SARS CoV_2 N protein detection (30). Thus, to make sensitive recognition 8 μ M
282 probe could be used for this model. Lastly, model 1.2 allowed effective hybridization on both
283 lines and this was resulted by clear line intensity and the lowest detection amount of target.

284
285 When compared to all models in terms of the LOD, the length of the target has crucial role for
286 LFA efficiency. It could be inferred from these results 50 base long target sequence could be
287 sensitively recognized compared to the 72 base long as the base length of target sequence
288 become shorter, LOD was observed as lower. This may be caused by the high probability of the
289 hairpin structures in long bases, which can interfere the hybridization on the assay. Therefore,
290 sensitive detection is closely related with the length of target sequence and hybridization models
291 between the target and capture reagents for LFA. Along with this, it should be highlighted that
292 the main gene length, 72 base long, is also clearly detected by developed strip assay models and
293 could be used for the detection of 2019-nCoV_N3.

294
295 Lastly, LFAs were also prepared by different times in order to see the stability of conjugates
296 and LFAs efficiency. Therefore, assays were applied by 6 months awaited conjugates. It was
297 found that conjugates are still stable and works efficiently in terms of the hybridization on the
298 LFAs and both lines on the strips were observed, clearly (data not shown). Since the stability
299 of the conjugates is also highly related with the red color of suspension they still have their
300 original color (data not shown). Therefore, designed LFAs with these models have potential for

301 long shelf life if they are fabricated. Because the developed method is also consistent in terms
302 of the reproducibility and there was no difference in batch to batch production or preparation
303 of all LFA strips.

304

305 As a conclusion, the detection of SARS-CoV-2 by targeting the 2019-nCoV_N3 gene region
306 was succeeded by designed LFAs models as a first study according to the best of our knowledge.

307 Although the detection of virus by LFAs is commonly based on the immunoglobulins of patients
308 or antigens these models are for the molecular detection of SARS-CoV-2 since it is the most
309 reliable method in the world. To highlight that designed LFAs are also cost effective as they are
310 naked eye analysis assays and need to conventional PCR products instead of the expensive
311 devices and reagents for analysis such as rRT-PCR. We believe that findings will be valuable
312 for various molecular detection methods for SARS-CoV-2 and its mutants. Because assay is
313 based on the hybridization and can be rapidly designed for specific sequences of mutant viruses.

314 Thus, the detection of either mutated or conserved regions could be possible by these type of
315 assay models. Since the PCR products were recognized and parameters were optimized in
316 designed LFAs they might also be a candidate for point of care diagnosis in terms of the
317 molecular detection of SARS-CoV-2 for further fabrication. In this perspective, applying the
318 developed LFAs to the real samples coming from the patients will be planned for the future
319 work.

320

321 **ACKNOWLEDGMENTS**

322 This work was supported by Inonu University Scientific Research Project (BAP; TOA-2020-
323 2238).

324

325 **REFERENCES**

- 326 1. Zhou, P., Yang, X.L., Wang, X.G., Hu, B., Zhang, L., Zhang, W., Si, H.R., Zhu, Y., Li,
327 B., Huang, C.L., Chen, H.D., Chen, J., and other 17 authors: A pneumonia outbreak
328 associated with a new coronavirus of probable bat origin, *Nature*, 579,270–273 (2020).
- 329 2. Ahmed, S.F., Quadeer, A.A., McKay, M.R.: Preliminary identification of potential
330 vaccine targets for the COVID-19 coronavirus (SARS-CoV-2) based on SARS-CoV
331 immunological studies, *Viruses*, 12, 254 (2020)
- 332 3. Kang, S., Yang, M., Hong, Z., Zhang, L., Huang, Z., Chen, X., He, S., Zhou, Z., Zhou,
333 Z., Chen, Q., Yan, Y., Zhan, C., and other 2 authors: Crystal structure of SARS-CoV-2
334 nucleocapsid protein RNA binding domain reveals potential unique drug targeting sites,
335 *Acta Pharm Sin B.*, 10,1228–1238 (2020).
- 336 4. Jung, Y., Park, G.S., Moon, J.H., Ku, K., Beak, S.H., Lee, C.S., Kim, S., Park, E.C., Park,
337 D., Lee, J.H., Byeon, C.W., Lee, J.J., and other 6 authors: Comparative analysis of primer–
338 probe sets for RT-qPCR of COVID-19 causative virus (SARS-CoV-2), *ACS Infect. Dis.*,
339 6,2513-2523 (2020).
- 340 5. Huang, C., Wang, Y., Li, X., Ren, L., Zhao, J., Hu, Y., Zhang, L., Fan, G., Xu, J., Gu, Xi.,
341 Cheng, Z., Yu, T., and other 17 authors: Clinical features of patients infected with 2019
342 novel coronavirus in Wuhan, China, *Lancet*, 395,497–506 (2020).
- 343 6. Yang, Y., Yang, M., Yuan, J., Wang, F., Wang, Z., Li, J., Zhang, M., Xing, L., Wei, J.,
344 Peng, L., Wong, G., Zheng, H., and other 9 authors: Comparative sensitivity of different
345 respiratory specimen types for molecular diagnosis and monitoring of SARS-CoV-2
346 shedding in COVID-19 patients, *Innovation*, 1:3 (2020).
- 347 7. Zhang, W., Du, R.H., Li, B., Zheng, X.S., Yang, X.L., Hu, B., Wang, Y.Y., Xiao, G.Fu.,
348 Yan, B., Shi, Z.L., Zhou, P.: Molecular and serological investigation of 2019-nCoV infected
349 patients: implication of multiple shedding routes, *Emerg Microbes Infect.*, 9,386–389

- 350 (2020).
- 351 8. Holshue, M.L., DeBolt, C., Lindquist, S., Lofy, K.H., Wiesman, J., Bruce, H., Spitters,
352 C., Ericson, K., Wilkerson, S., Tural, A., Diaz, G., Cohn, A., and other 12 authors: First
353 Case of 2019 Novel Coronavirus in the United States, *N Engl J Med.*, 382, 929–936 (2020).
- 354 9. Pan, Y., Zhang, D., Yang, P., Poon, L.L.M., Wang, Q.: Viral load of SARS-CoV-2 in
355 clinical samples, *Lancet Infect Dis.*, 20, 411–412 (2020).
- 356 10. Wang, X., Liu, L.H., Ramstroem, O., Yan, M.: Engineering Nanomaterial Surfaces for
357 Biomedical Applications, *Exp Biol Med.*, (Maywood) 234, 1128–1139 (2009).
- 358 11. Martínez-Paredes, G., González-García, M.B., Costa-García, A.: Genosensor for SARS
359 virus detection based on gold nanostructured screen-printed carbon electrodes,
360 *Electroanalysis*, 21,379-385 (2009).
- 361 12. Mahari, S., Roberts, A., Shahdeo, D., Gandhi, S.: eCovSens-Ultrasensitive Novel In-
362 House Built Printed Circuit Board Based Electrochemical Device for Rapid Detection of
363 nCovid-19 antigen, a spike protein domain 1 of SARS-CoV-2, *BioRxiv.*, (2020). doi:
364 <https://doi.org/10.1101/2020.04.24.059204> (available online 19 October 2022)
- 365 13. Roberts A., Mahari, S., Shahdeo, D., Gandhi.: Label-free detection of SARS-CoV-2
366 Spike S1 antigen triggered by electroactive gold nanoparticles on antibody coated fluorine-
367 doped tin oxide (FTO) electrode, *Analytica Chimica Acta.*, 1188, 339207 (2021).
- 368 14. Shahdeo, D., Roberts, A., Archana G.J., Shrikrishna, S.N., Mahari, S., Nagamani, K.,
369 Gandhi, S.: Label free detection of SARS CoV-2 Receptor Binding Domain (RBD) protein
370 by fabrication of gold nanorods deposited on electrochemical immunosensor, *Biosensors*
371 *and Bioelectronics*, 212, 114406 (2022).
- 372 15. Shahdeo, D., Chauhan, N., Majumdar, A., Ghosh, A., Gandhi, S.: Graphene-Based

- 373 Field-Effect Transistor for Ultrasensitive Immunosensing of SARS-CoV-2 Spike S1
374 Antigen, *ACS Appl. Bio Mater.*, 5:7, 3563–3572 (2022).
- 375 16. Ligieroa, C.B.P., Fernandes, T.S., D'Amato, D.L., Gaspar, F.V., Duarte, P.S., Strauch,
376 M.A., Fonseca, J.G., Meirelles, L.G.R., Silva, P.B., Azevedo, R.B., Martins, G.A.S.,
377 Archanjo, B.S., and other 4 authors: Influence of particle size on the SARS-CoV-2 spike
378 protein detection using IgG-capped gold nanoparticles and dynamic light scattering, *Mater.*
379 *Today Chem.*, 25, 100924 (2022).
- 380 17. DaSilva, P.B., DaSilva, J.R., Rodrigues, M.C., Vieira, J.A., Andrade, I.A., Nagata, T.,
381 Santos, A.S.: Detection of SARS-CoV-2 virus via dynamic light scattering using antibody-
382 gold nanoparticle bioconjugates against viral spike protein, *Talanta*, 243, 123355 (2022).
- 383 18. Ang, G.Y., Yu, C.Y., Yean, C.:Y. Ambient temperature detection of PCR amplicons with
384 a novel sequence-specific nucleic acid lateral flow biosensor, *Biosensors & bioelectronics.*,
385 38,151–156 (2012).
- 386 19. Reboud, J., Xu, G., Garrett ,A., Adriko, M., Yang, Z., Tukahebwa, E.M., Rowell, C.,
387 Cooper, J.M.: Paper-based microfluidics for DNA diagnostics of malaria in low resource
388 underserved rural communities, *Proc Natl Acad Sci USA.*, 116,4834–4842 (2019).
- 389 20. Glynou, K., Ioannou, P.C., Christopoulos, T.K., Syriopoulou, V.: Oligonucleotide-
390 Functionalized Gold Nanoparticles as Probes in a Dry-Reagent Strip Biosensor for DNA
391 Analysis by Hybridization, *Anal Chem.*, 75, 4155–4160 (2003).
- 392 21. Li, Z., Yi, Y., Luo, X., Xiong, N., Liu, Y., Li, S., Sun, R., Wang, Y., Hu, B., Chen, W.,
393 Zhang, Y., Wang, J., and other 12 authors: Development and Clinical Application of A
394 Rapid IgM-IgG Combined Antibody Test for SARS-CoV-2 Infection Diagnosis, *J Med*
395 *Viro.*, 92, 1518–1524 (2020).

- 396 22. Dimov, I.K., Garcia-Cordero, J.L., O'Grady, J., Poulsen, C.R., Viguier, C., Kent, L.,
397 Daly, P., Lincoln, B., Maher, M., O'Kennedy, R., Smith, T.J., Ricco, A.J., and other 1 author:
398 Integrated microfluidic tmRNA purification and real-time NASBA device for molecular
399 diagnostics., *Lab on a chip*, 8,2071–2078 (2008).
- 400 23. Lucia, C., Federico, P.B., Alejandra, G.C.: An ultrasensitive, rapid, and portable
401 coronavirus 2 SARS-CoV-2 sequence detection method based on CRISPR-Cas12, *BioRxiv*
402 (2020). doi: <https://doi.org/10.1101/2020.02.29.971127> (available online 19 October 2022)
- 403 24. Broughton, J.P., Deng, X., Yu, G., Fasching, C.L., Servellita, V., Singh, J., Miao, X.,
404 Streithorst, J.A., Granados, A., Gonzalez, A.S., Zorn, K., Gopez, A., and other 8 authors:
405 CRISPR–Cas12-based detection of SARS-CoV-2, *Nat Biotechnol.*, 38,870–874 (2020).
- 406 25. Grabar, K.C., Freeman, R.G., Hommer, M.B., Natan, M.J.: Preparation and
407 characterization of Au colloid monolayers, *Anal Chem.*, 67,735-743 (1995).
- 408 26. Cam, D., Oktem, H.A.: Development of rapid dipstick assay for food pathogens,
409 *Salmonella*, by optimized parameters, *J Food Sci Technol.*, 56,140–148 (2019).
- 410 27. Zhao, W., Brook, M.A., Li, Y.: Design of gold nanoparticle-based colorimetric
411 biosensing assays, *Chembiochem.*, 9:15, 2363-71 (2008).
- 412 28. Jauset-Rubio, M., Svobodová, M., Mairal, T., McNeil, C., Keegan, N., Saeed, A., Abbas,
413 M.N., El-Shahawi, M.S., Bashammakh, A.S., Alyoubi, A.O., O'Sullivan, C.K.,:
414 Ultrasensitive, rapid and inexpensive detection of DNA using paper based lateral flow assay,
415 *Sci Rep.*, 6, 37732 (2016).
- 416 29. Baeumner, A.J., Pretz, J., and Fang, S.: A Universal Nucleic Acid Sequence Biosensor
417 with Nanomolar Detection Limits, *Anal. Chem.*, 76: 4, 888–894 (2004).
- 418 30. Grant, B.D., Anderson, C.E., Williford, J.R., Alonzo, L.F., Glukhova, V.A., Boyle, D.S.,

419 Weigl, B.H., Nichols, K.P.: SARS-CoV-2 Coronavirus Nucleocapsid Antigen-Detecting
420 Half-Strip Lateral Flow Assay Toward the Development of Point of Care Tests Using
421 Commercially Available Reagents, *Analytical Chemistry*, 92:16, 11305-11309 (2020).

422 **Figures Legends**

423 Figure 1. LFAs developed by M170 (A, B) and M120 (C, D) membrane using model 1A (A, C)
424 and model 1B (B,D) at 37°C drying. Strips A1-A5; B1-B5; C1-C2; D1-D2 were prepared by
425 4µM probe and strips A6-A10; B6-B10; C3-C4; D3-D4 were prepared by 8µM probe. target:
426 2019-nCoV_N3 (72 bp), SSC: running buffer. Arrows show the test and control lines.

427
428 Figure 2. Application of PCR products to LFAs developed by two types of membranes and three
429 models. Strips 1-8 were prepared by 4µM and strips 9-16 were prepared by 8µM. Strips 1-15
430 were prepared by M170 and strip 16 was prepared by M120 membrane. Strips 1-5: model 1.2,
431 Strips 6-13,16: model 1B, strips 14-15: model 1A. Non heated: Non heated PCR product.
432 Se20_60 bio, Crn2SH, Mers CoV_N2, Mers CoV_N3 and RdRp/Orf1 and SSC are negative
433 controls. Arrows show the test lines.

434
435 Figure 3. LOD of target by model 1A using M170 (A-B) and M120 (C-E). A) 0.5µM, B) 0.1µM,
436 C) 0.5µM, D) 0.1µM, E) 0.005µM target. Strips 1-2 were prepared by 4µM probe and strips 3-
437 4 were by 8µM. Strip E1 was prepared by 4µM and E2 was by 8µM, and then target was applied
438 to both. All 1-3 strips were applied by target and strips 2-4 were by buffer as a negative control.
439 Arrows show the test and control lines.

440
441 Figure 4. LOD of target by model 1B using M170 (A-C) and M120 (D-G). A) 0.5µM, B) 0.1µM,
442 C) 100pM, D) 0.5µM, E) 0.1µM, F) 0.005µM, G) 100Pm target. Strips 1-2 were prepared by
443 4µM probe and strips 3-4 were by 8µM. Strips F1-F2 were prepared by 8µM. All 1-3 strips

444 were applied by target and strips 2-4 were by buffer as a negative control. Arrows show the test
445 lines.

446
447 Figure 5. LOD of target by model 1.2 using M170 (A-C) and M120 (D-F). A) 0.005 μ M, B)
448 50pM, C) 5pM, D) 0.005 μ M, E) 100pM, F) 50pM target. Strips 1-2 were prepared by 4 μ M
449 prob and strips 3-4 were by 8 μ M. Strips C1-C2 were prepared by 8 μ M. All 1-3 strips were
450 applied by target and strips 2-4 were by buffer as a negative control. Arrows show the test lines.

451

452 **Supplementary Figures**

453 Fig. S1. UV-Vis Spectroscopy (A), Dynamic Laser Particle Size Analyzer (B) and STEM
454 analysis (C) of synthesized AuNPs

455

456 Fig. S2. The UV-Vis spectra of AuNPs after the surface modifications with probes. A) Prob 1A
457 prepared by 4 μ M probe B) Prob 1A prepared by 8 μ M probe C) Prob 1B prepared by 4 μ M probe
458 D) Prob 1B prepared by 8 μ M probe E) Prob 1.2 prepared by 4 μ M probe F) Prob 1.2 prepared
459 by 8 μ M probe

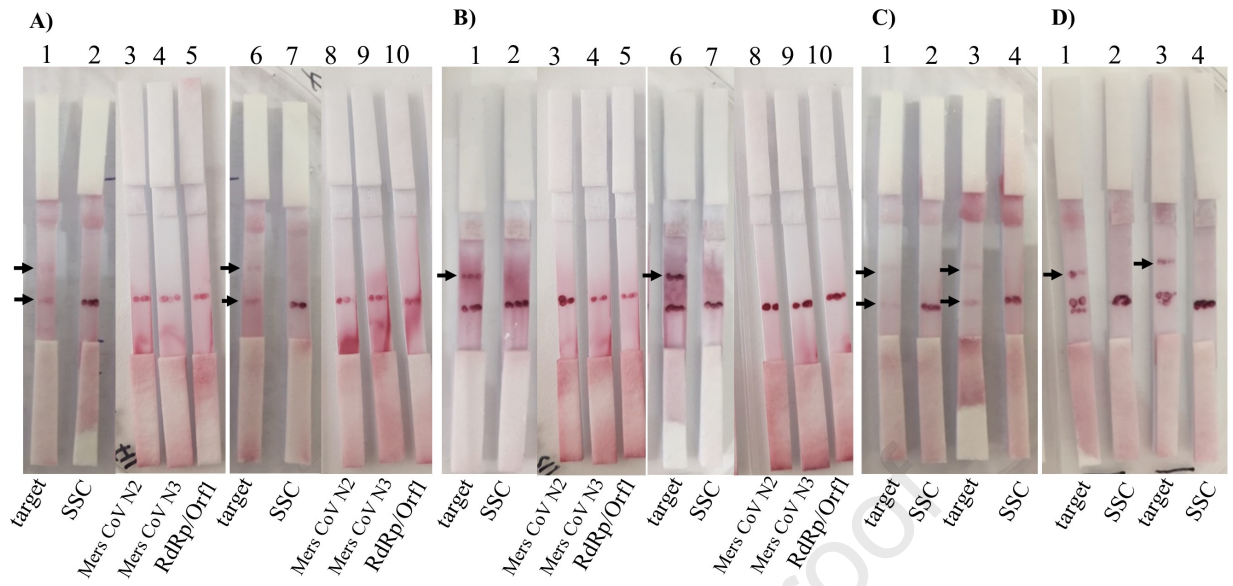
460

461 Fig. S3. LFA sandwich models for the detection of SARS-CoV-2 N gene region. 1A and 1B is
462 designed for 72 base long N gene (2019-nCoV_N3) and 1.2 is for 50 base long N gene (2019-
463 nCoV_N3). COVID-19 N gene: 2019-nCoV_N3

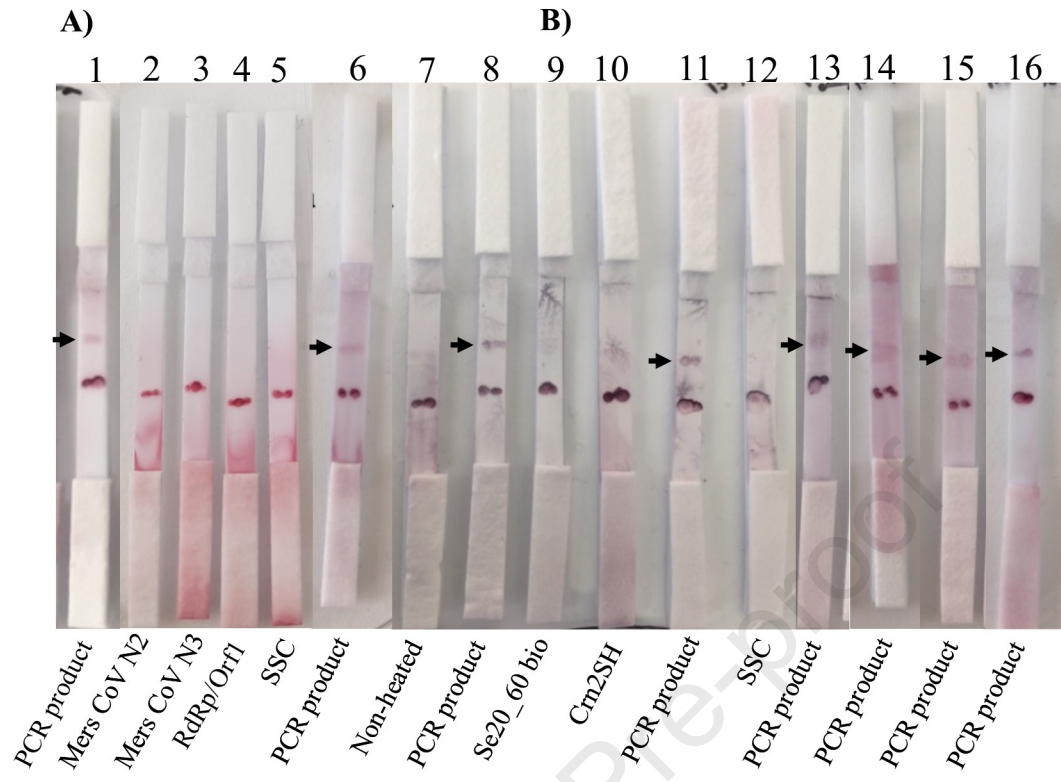
464

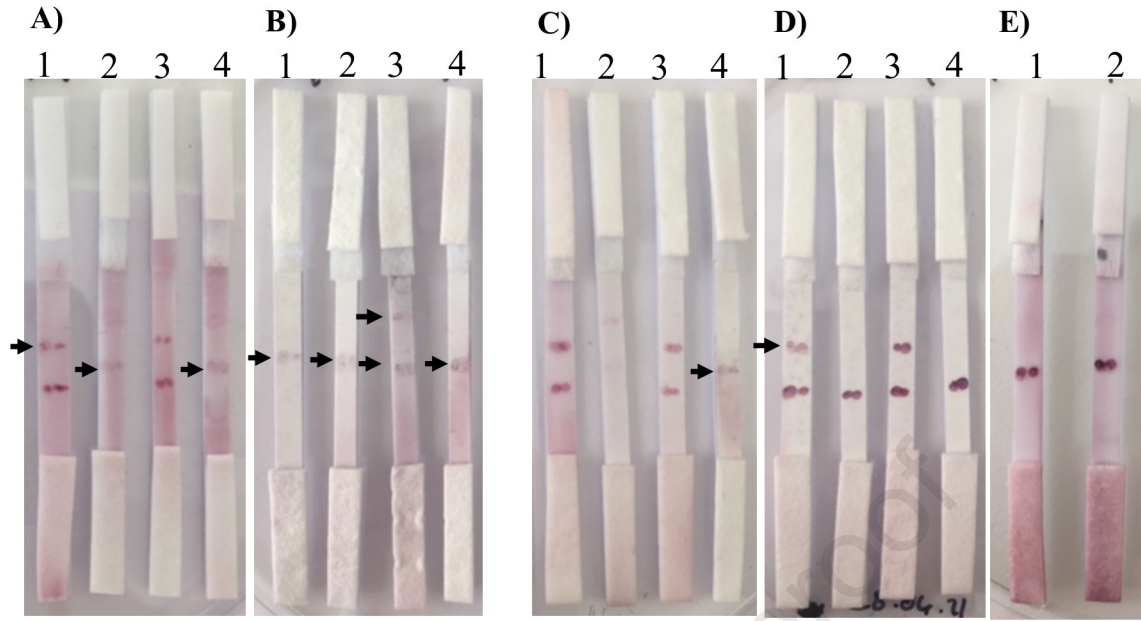
465 Fig. S4. Agarose gel electrophoresis of 2019-nCoV_N3. 1) Ultra low DNA ladder
466 (Thermoscientific), 2-9) PCR products of 2019-nCoV_N3 (72 bp).

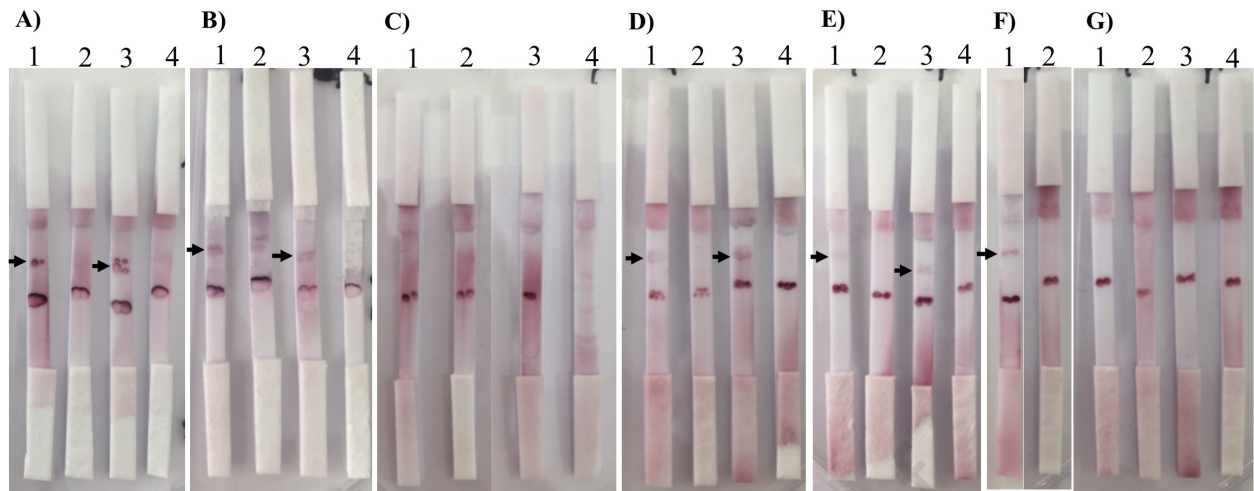
467

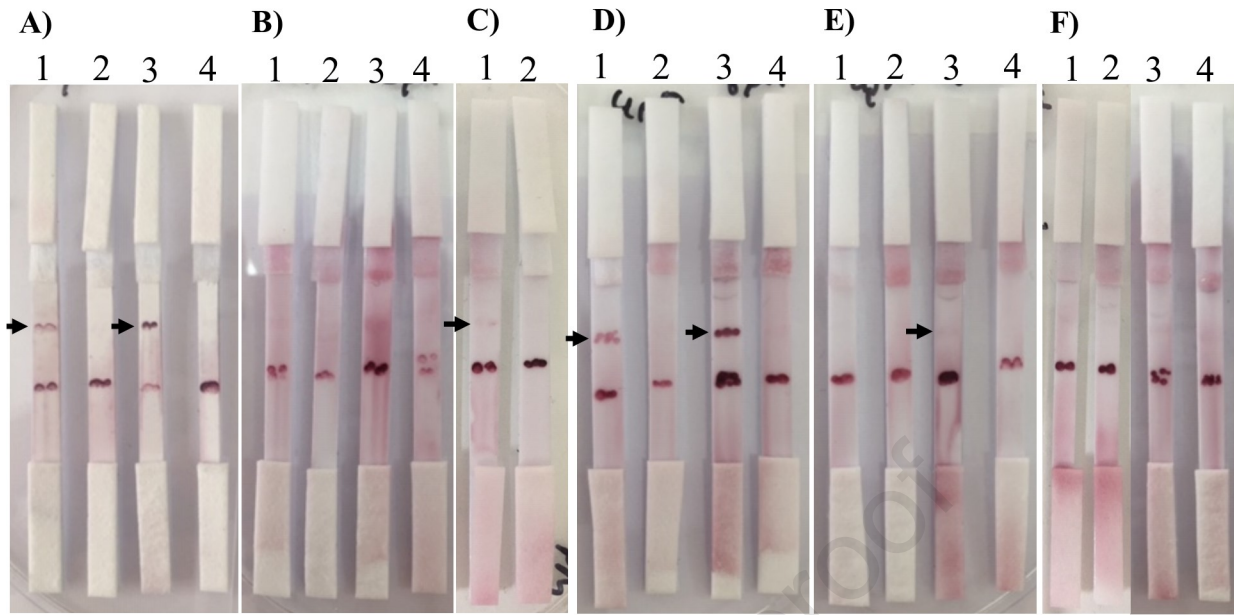


Journal Pre-proof









Highlights

- 2019-nCoV_N3 was detected by developed LFA, rapidly
- This is the first sandwich assay shows the hybridization models of PCR products for the detection of 2019-nCoV_N by LFA
- Developed LFAs can be an alternative method to the conventional and real time PCR
- Designed LFAs can be adoptable to the molecular detection of SARS-CoV-2 mutants